

# CHEMISTRY

## A **European** Journal

### Supporting Information

#### **Mechanistic Insights into Growth of Surface-Mounted Metal-Organic Framework Films Resolved by Infrared (Nano-) Spectroscopy**

Guusje Delen<sup>+</sup>, Zoran Ristanović<sup>+</sup>, Laurens D. B. Mandemaker, and Bert M. Weckhuysen<sup>\*[a]</sup>

chem\_201704190\_sm\_miscellaneous\_information.pdf

## Supporting Information

### S1. Infrared reflection absorption spectroscopy

#### 1. Direct synthesis mixtures

The IRRAS spectra in Figure 2c were measured by recording separately absorbance from CuAc<sub>2</sub>, btc, and btc upon addition of CuAc<sub>2</sub>. The spectra were recorded from a solid phase, upon ethanol evaporation. In this way, we observed the formation of vibrations characteristic for [Cu<sub>3</sub>(btc)<sub>2</sub>]. For measuring the stoichiometric series of CuAc<sub>2</sub>+btc solutions (Fig. S2), 1 mM ethanolic solutions of CuAc<sub>2</sub> and btc were mixed in different ratios of reactants (i.e., Cu:btc = 3:2, 10:1, 5:1, and 1:5 molar ratios) for 2 min. The solutions were drop-casted on a clean Au wafer and allowed to dry. IRRAS spectra were typically recorded 3-5 min after ethanol evaporation.

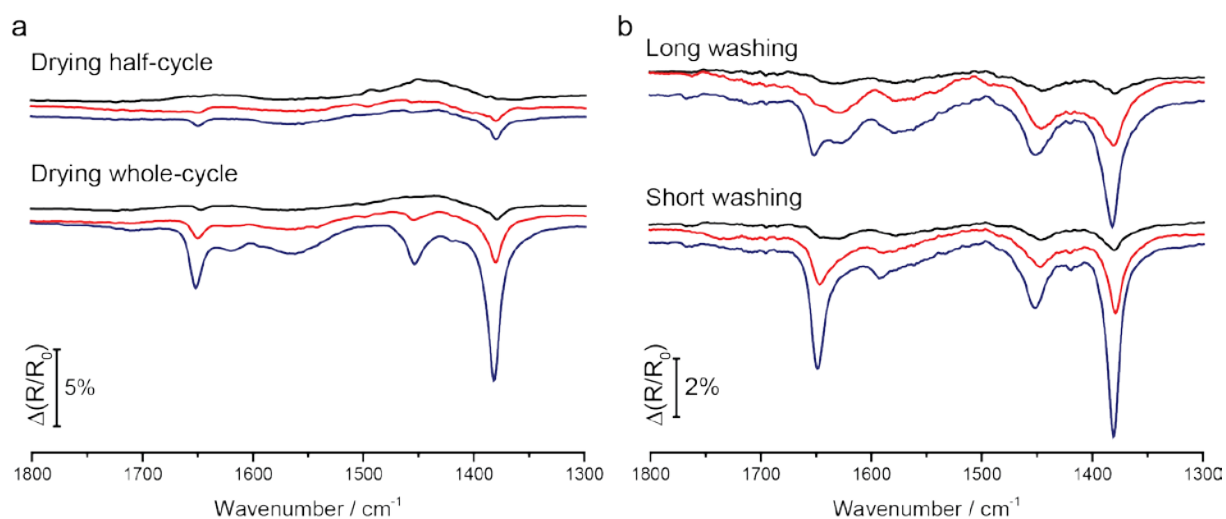


**Figure S1.** IRRAS spectra of control experiments performed to verify the effect of drying (a) and washing (b) on SURMOF growth. Analogue to the samples described in the manuscript, SURMOFs were grown by alternatingly placing an MHDA functionalized Au/Si substrate in a 1mM  $\text{CuAc}_2$  solution and a 1 mM btc solution for 10 and 20 min, respectively, with washing steps between growth phases. This sequence constitutes one deposition cycle. Samples corresponding to the spectra shown in (a) were washed for 10 s in ethanol and were dried either after each half cycle (top) or each whole cycle (bottom). In the experiments for (b), samples were either washed for a long time (5 min in flowing EtOH) or for a short time (10 s) and were dried after each whole cycle. This Figure shows the detrimental effect of drying each half cycle on SURMOF growth, whereas the length of the washing step was shown to have little influence.

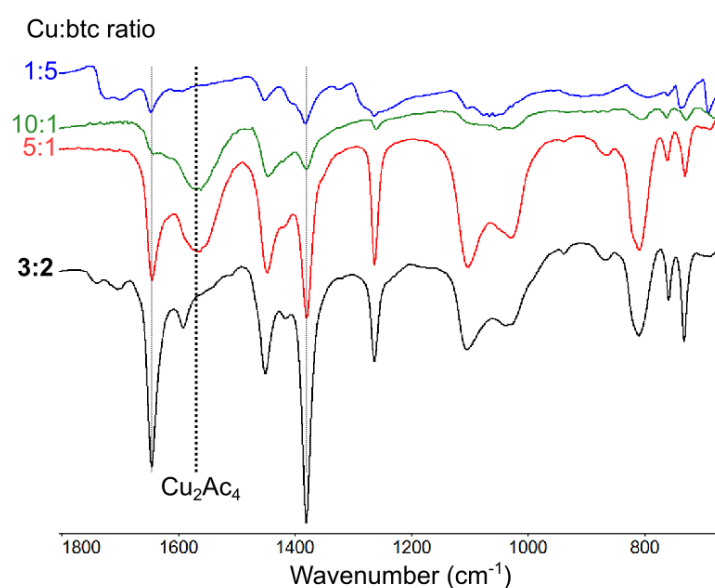


**Figure S2.** IRRAS spectra of  $\text{CuAc}_2$ /btc mixtures with different molar ratios of Cu: btc, recorded after evaporation of ethanol, approximately 5 min upon mixing 1 mM solutions of reactants. The

disappearance of the paddle-wheel  $[\text{Cu}_2\text{Ac}_4]$  species at  $1580\text{ cm}^{-1}$  with increasing btc concentration is visible.

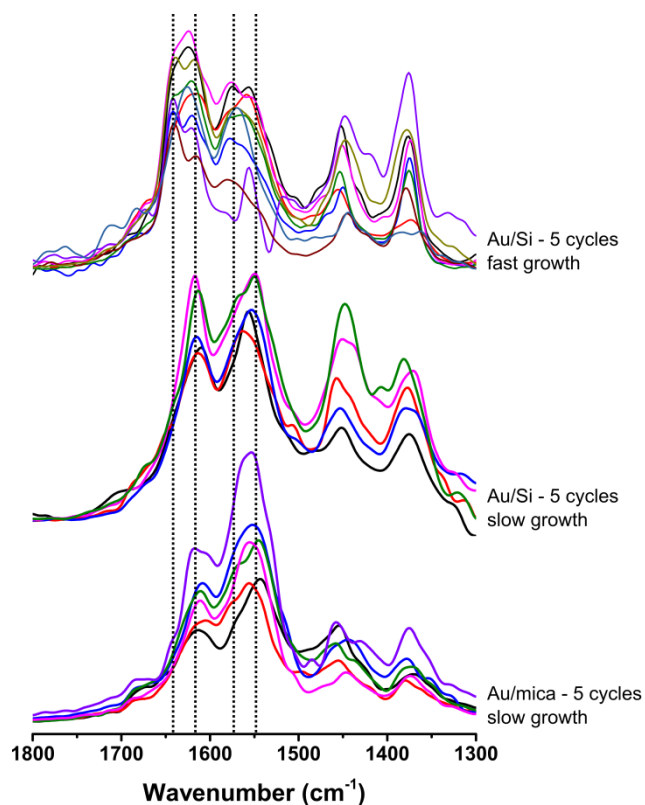


**Figure S3.** Examples of AFM-nano-IR spectra recorded at different locations of differently grown SURMOF films. Note that the band at  $1640\text{ cm}^{-1}$  arises only in the fast growth samples.

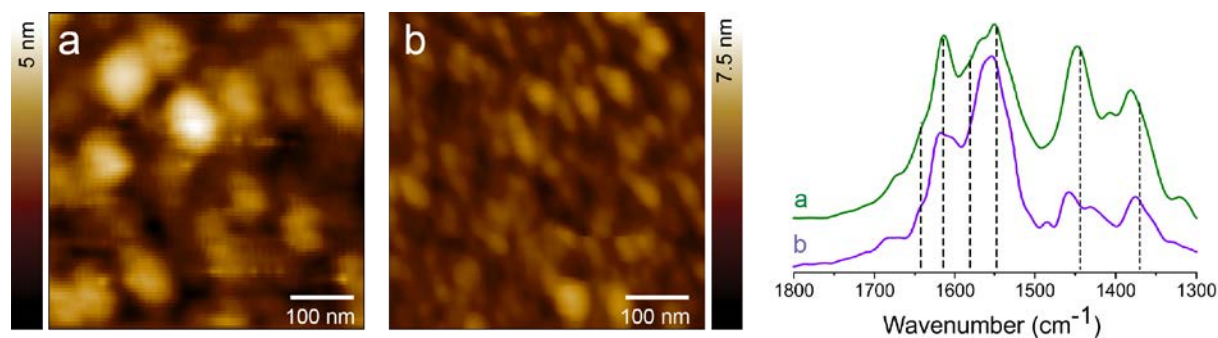


**Figure S4.** AFM images of 5 layer SURMOF samples on Au/Si (a) and Au/mica (b) grown via manual synthesis with half-cycle drying indicating decreased growth rates as a result of washing and drying steps. IR spectra on the right show the formation of HKUST-1 with a characteristic paddlewheel structure. Images were smoothed by using either a Gaussian filter (a, 2 pixel size) and a Median filter (b, 6 pixel size).

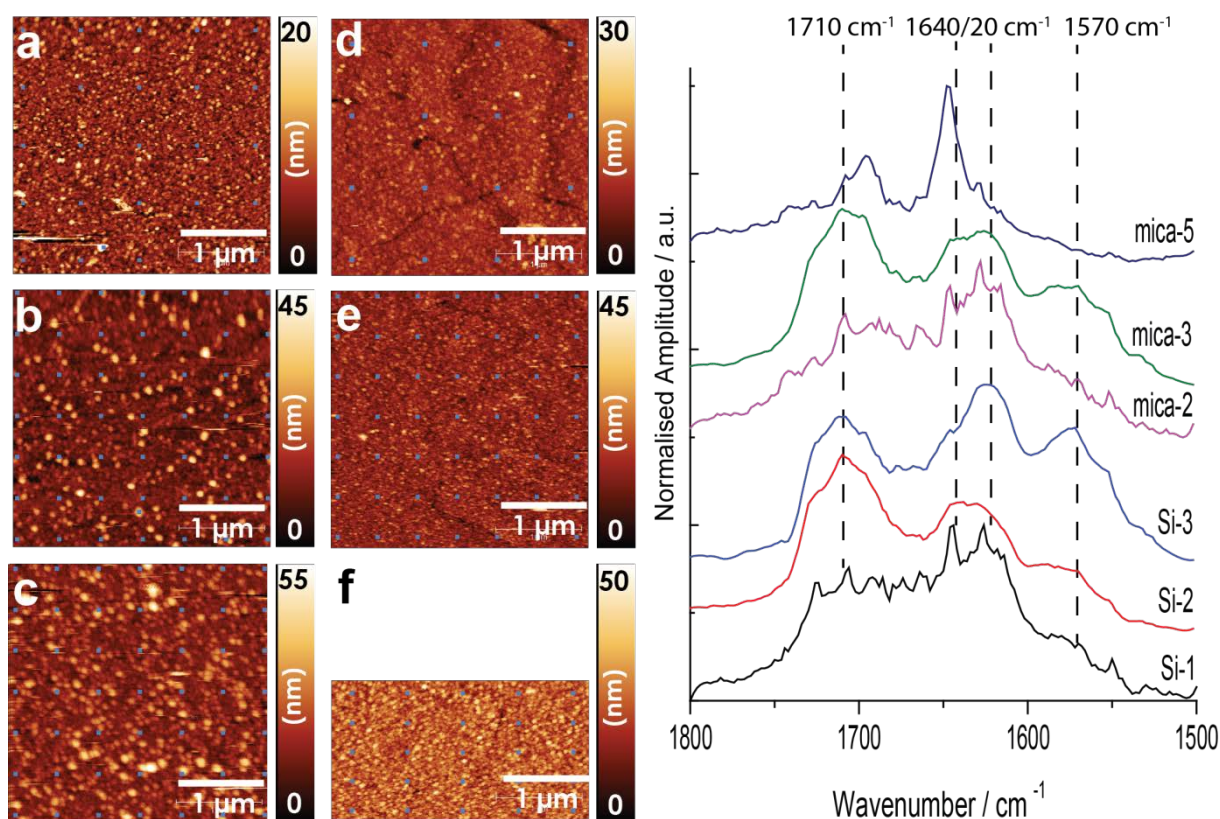


**Figure S5.** Series of AFM images and their average spectra for different films grown with manual synthesis with drying each whole cycle. The left panel shows AFM images with array positions (blue squares) for IR measurements with their corresponding averaged spectrum displayed on the right. a-c) 1, 2 and 3 cycles of HKUST-1 on Au/Si, respectively and d-f) 2,3 and 5 cycles of HKUST-1 on Au/mica, respectively. A peak at 1710 cm<sup>-1</sup> most likely corresponds to COOH vibration of MHDA, which was visible due to signal enhancement between the Au substrate and a gold tip used in AFM-IR contact measurement mode. Note that non-linear near-field enhancements may occur when scanning nm-thick organic layers. These AFM-nano-IR measurements were performed at ORNL.

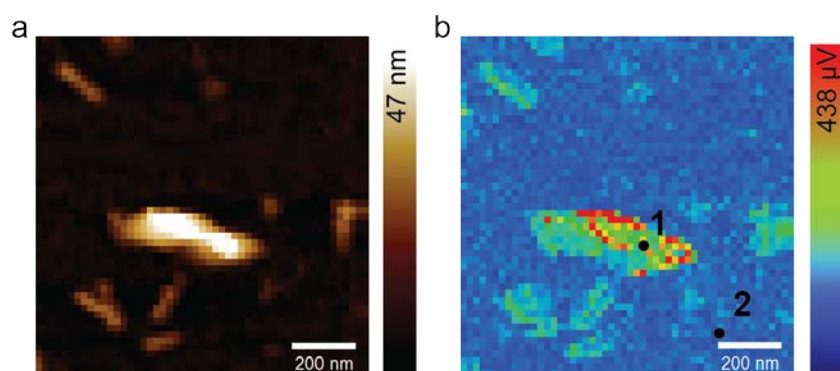


**Figure S6.** Magnifications of Fig. 4a-b. A) AFM topology and b) AFM-IR intensity map at 1450 cm<sup>-1</sup>. The magnifications clearly show the overlap of topology and IR signal. Markers 1 and 2 indicate IR spectrum sampling positions corresponding to spectra shown in Fig. 4e.

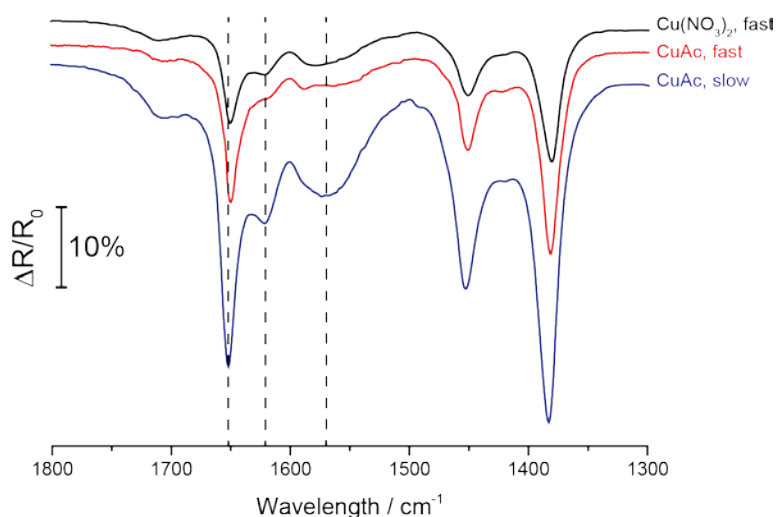


**Figure S7.** IRRAS spectra of three SURMOFs grown by different automated syntheses, also shown in Fig.5 . Quantitatively, IRRAS confirms a variation in growth rates which was also shown using AFM (Fig.5 b-d). Quality of films grown by  $\text{CuAc}_2$ , determined by the degree of Cu-paddlewheel substitution, is increased for fast grown films.

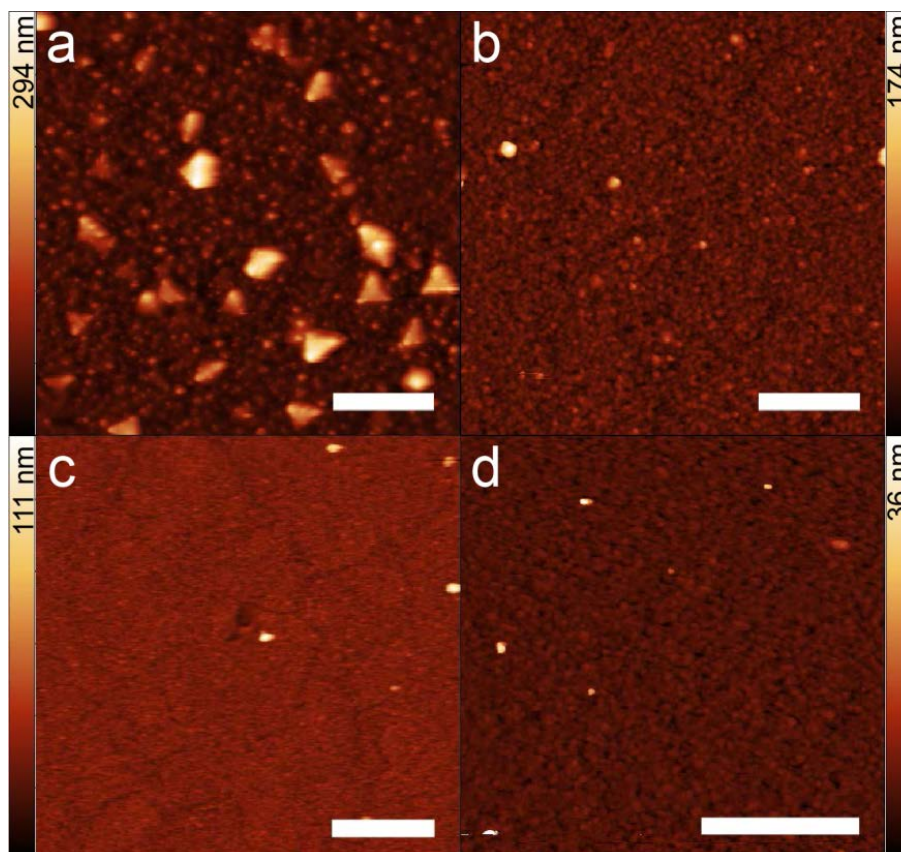


**Figure S8.** AFM images of 50 layers HKUST-1 grown by different synthesis (precursor, procedure) and on different substrates. Root mean-square roughness values (rms) are provided as a guideline for the film smoothness. a) Slow synthesis procedure 1 using  $\text{CuAc}_2$  on Au/mica, rms= 32.7 nm; b) fast synthesis procedure 2 using  $\text{CuAc}_2$  on Au/mica, rms= 8.7 nm; c) fast synthesis procedure 2 using

$\text{Cu}(\text{NO}_3)_2$  on Au/mica, rms= 4.0 nm and d) bare Au/mica, rms= 1.4 nm. Clear influence of synthesis parameters can be seen on the growth of large irregular features instead of uniform films. All scale bars are 1  $\mu\text{m}$ .